DOI:10.1111/j.1365-2125.2005.02483.x

Prediction of *in vivo* drug–drug interactions from *in vitro* data: impact of incorporating parallel pathways of drug elimination and inhibitor absorption rate constant

Hayley S. Brown, Kiyomi Ito,[1] Aleksandra Galetin & J. Brian Houston

School of Pharmacy & Pharmaceutical Sciences, University of Manchester, Manchester, UK, and [1]Department of Clinical Pharmacokinetics, Hoshi University, Tokyo, Japan

.

Correspondence
Professor J. Brian Houston, School of Pharmacy and Pharmaceutical Sciences, University of Manchester, Manchester M13 9PL, UK.
Tel: + 44 (0)161 275 2358
Fax: + 44 (0)161 275 8349
E-mail: brian.houston@manchester.ac.uk

Keywords
CYP2C9, CYP2D6, CYP3A4, drug–drug interactions, *in vitro* prediction

Received
4 March 2005
Accepted
15 June 2005

Aims
Success of the quantitative prediction of drug–drug interactions via inhibition of CYP-mediated metabolism from the inhibitor concentration at the enzyme active site ([*I*]) and the *in vitro* inhibition constant (K_i) is variable. The aim of this study was to examine the impact of the fraction of victim drug metabolized by a particular CYP (f_{mCYP}) and the inhibitor absorption rate constant (k_a) on prediction accuracy.

Methods
Drug–drug interaction studies involving inhibition of CYP2C9, CYP2D6 and CYP3A4 (n = 115) were investigated. Data on f_{mCYP} for the probe substrates of each enzyme and k_a values for the inhibitors were incorporated into *in vivo* predictions, alone or in combination, using either the maximum hepatic input or the average systemic plasma concentration as a surrogate for [*I*]. The success of prediction (AUC ratio predicted within twofold of *in vivo* value) was compared using nominal values of f_{mCYP} = 1 and k_a = 0.1 min^{-1}.

Results
The incorporation of f_{mCYP} values into *in vivo* predictions using the hepatic input plasma concentration resulted in 84% of studies within twofold of *in vivo* value. The effect of k_a values alone significantly reduced the number of over-predictions for CYP2D6 and CYP3A4; however, less precision was observed compared with the f_{mCYP}. The incorporation of both f_{mCYP} and k_a values resulted in 81% of studies within twofold of *in vivo* value.

Conclusions
The incorporation of substrate and inhibitor-related information, namely f_{mCYP} and k_a, markedly improved prediction of 115 interaction studies with CYP2C9, CYP2D6 and CYP3A4 in comparison with $[I]/K_i$ ratio alone.

Introduction

Drug–drug interactions resulting from inhibition of CYP-mediated metabolism can lead to serious toxicities, and have resulted in a number of compounds being withdrawn from the market. In recent years there has been an increased use of various *in vitro* systems used to detect CYP inhibition, which is qualitatively a useful tool. However, the extrapolation of these *in vitro* data to ultimately provide a quantitative *in vivo* prediction is problematic, and at present there is no comprehensive strategy that allows for the identification of particular drugs at risk from an inhibitory interaction [1–5].

In human *in vivo* interaction studies, the degree of interaction is expressed as the ratio of the area under the plasma concentration–time curve (AUC) in the presence and absence of an inhibitor. For many, but not all, cases this involves multiple oral dosing and the assumption is made that a new steady state is achieved. Also, for simplicity other conditions are commonly assumed: the victim drug is administered orally, cleared exclusively by the liver by way of a single metabolic pathway and the 'well-stirred' liver model applies. The AUC ratio is related to the ratio of the metabolic intrinsic clearance (CL_{int}) as described by equation 1. The drug concentration *in vivo* is usually much lower than the K_m value and the mechanism of inhibition (competitive or noncompetitive) is not relevant; therefore, equation 1 is valid for both inhibition types.

$$\frac{AUC_i}{AUC} = \frac{CL_{int}}{CL_{int,i}} = 1 + \frac{[I]}{K_i} \quad (1)$$

where $[I]$ is the inhibitor concentration available to the enzyme and subscript i indicates the presence of the inhibitor.

We have previously constructed a database of 146 studies to evaluate the prediction of drug–drug interactions involving reversible inhibition of CYP2C9, CYP2D6 and CYP3A4 [6]. In this analysis, we evaluated the utility of the $[I]/K_i$ ratio by using various inhibitor plasma concentrations as surrogates for $[I]$. Results from this database analysis showed that the greatest change in AUC was observed for CYP3A4 (approximately 24-fold increase), followed by CYP2D6 (approximately 11-fold increase), with a fivefold AUC increase for CYP2C9 studies. The interaction studies involved nine different substrates for CYP2C9, 13 substrates for CYP2D6, with 18 substrates for CYP3A4 as shown in Figure 1, together with the predicted relationship based on equation 1. Using the maximum hepatic input concentration as $[I]$ together with the *in vitro* K_i value was found to be the most successful method for categorizing CYP inhibitors and for identifying true negative drug–drug interactions. Although false negatives were eliminated, several false positives were evident and most true positives were markedly overpredicted (Figure 1). It was concluded that this generic approach provides only an initial discriminating screen, since there are a number of specific factors related to both the substrate and inhibitor that will affect the *in vivo* predictions.

Predictions made using equation 1 assume that the fraction of substrate metabolized by way of the inhibited CYP pathway ($f_{m\mathrm{CYP}}$) is equal to 1. However, parallel

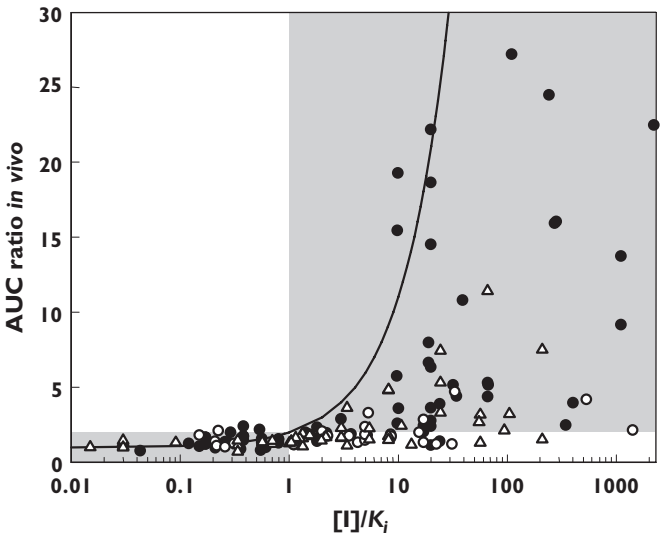

Figure 1
Relationship between the observed AUC ratio and the $[I]_{in}/K_i$ ratio for 146 drug–drug interactions involving CYP2C9 (○), CYP2D6 (△) and CYP3A4 (●). The line shown is the theoretical relationship based on equation 1. The shaded areas represent the regions corresponding to negative and positive drug–drug interactions as defined by the borderlines of an AUC ratio of 2 and an $[I]/K_i$ of 1 [2]

pathways of metabolism and renal clearance of unchanged drug will affect the $f_{m\mathrm{CYP}}$ and, consequently, the predicted degree of interaction, as even minor changes in the $f_{m\mathrm{CYP}}$ value (e.g. from 1 to 0.98) may alter predictions significantly [7]. Equation 2 can be used in the prediction of the *in vivo* AUC ratio when $f_{m\mathrm{CYP}}$ values are known and the other CYP pathways involved in the metabolism of the substrate are not subject to inhibition [7, 8]. Previously, we have demonstrated a substantial improvement in the quantitative predictions of drug–drug interactions involving CYP2D6 substrates using equation 2 rather than equation 1 [7].

$$\frac{AUC(+inhibitor)}{AUC(control)} = \frac{1}{\frac{f_{m\mathrm{CYP}}}{1+[I]/K_i} + (1 - f_{mCYP})} \quad (2)$$

Previously [6], we investigated the use of the maximum hepatic inhibitor concentration at the inlet to the liver ($[I]_{in}$). Calculation of this parameter (equation 3) relies on information on hepatic blood flow (Q_H), inhibitor dose (D), fraction absorbed from the gastrointestinal tract (f_a), the absorption rate constant (k_a) to provide an absorption term and the average systemic plasma concentration ($[I]_{av}$).

$$[I]_{in} = [I]_{av} + \frac{k_a \cdot f_a \cdot D}{Q_H} \quad (3)$$

In vivo clinical studies frequently do not report k_a values; in the absence of this information and in order to avoid false-negative prediction and obtain the largest $[I]_{in}$, it has been suggested that maximum k_a of 0.1 min^{-1} is appropriate, assuming the gastric emptying is the rate limiting step for absorption [9].

The aim of the present study was to extend the previous database analysis [6] on 146 reversible drug–drug interaction studies and investigate the impact of substrate- and inhibitor-related parameters, namely $f_{m\mathrm{CYP}}$ and k_a, on the prediction accuracy, using either $[I]_{av}$ or $[I]_{in}$ together with published K_i data. Values for $f_{m\mathrm{CYP}}$ were assigned for the commonly used substrate probes for CYP2C9, CYP2D6 and CYP3A4. In addition, k_a values were estimated for each CYP inhibitor and the significance of these values on the $[I]_{in}$ value and *in vivo* predictions were assessed. The effects of $f_{m\mathrm{CYP}}$ and k_a, alone and in combination, have been analysed in order to maximize the drug–drug interaction prediction accuracy.

Methods

Data collection

Drug–drug interaction studies involving the reversible inhibition of CYP2C9, CYP2D6 and CYP3A4 ($n = 146$) were obtained from published literature [6]. The degree of interaction in each study was expressed as the fold increase in the AUC in the presence of an inhibitor, compared with the control study. *In vitro* K_i values for the CYP inhibitors involved in the above studies were also collected from the literature. In most cases *in vitro* data were available for the same substrate as used in the *in vivo* study, and when several human liver microsomal studies had been conducted, average K_i values were used for the prediction. If there were no available *in vitro* data involving the *in vivo* substrate in question, then *in vitro* data from alternative, well-established probe substrates of that particular enzyme were used [6]. For example, in the absence of *in vitro* studies involving fluconazole and phenytoin, the K_i value obtained with (S)-warfarin was used.

Values of $f_{m\mathrm{CYP}}$ for each substrate were assigned using various literature data for a subset of 115 studies from the original database. The $f_{m\mathrm{CYP}}$ value for the CYP2C9 substrate tolbutamide was obtained by calculating the difference between the urinary recovery of metabolites in both the presence and absence of the CYP2C9 selective inhibitor sulphaphenazole (phenocopying). Phenotyping data obtained from extensive and poor metabolizers of CYP2D6 were used to calculate the $f_{m\mathrm{CYP}}$ values for these substrates [7]. A similar rationale was used to calculate the CYP2C19 contribution to phenytoin clearance and hence the $f_{m\mathrm{CYP}}$ value for CYP2C9. For warfarin, an $f_{m\mathrm{CYP}}$ value was calculated from a combination of urinary recovery of metabolites, biliary excretion and the recovery of unchanged drug as previously documented [10].

The $f_{m\mathrm{CYP}}$ values are shown in Table 1; as the assignment of $f_{m\mathrm{CYP}}$ values for CYP3A4 substrates was problematic, a range is shown for certain substrates. For all nine CYP3A4 substrates, the fraction excreted unchanged in urine is available and this provided an initial value for $f_{m\mathrm{CYP}}$ based on the assumption that all metabolism is mediated via CYP3A4. In some cases this may be an upper estimate and further clarification is required. For the three benzodiazepines (midazolam, triazolam or alprazolam) this was achieved by adopting a regression approach [7] using equation 2 and the AUC ratio and $[I]/K_i$ ratio for each substrate dataset ($n = 8$–

Table 1
Values of $f_{m\mathrm{CYP}}$ for the probe substrates in the *in vivo* interactions with CYP2C9, CYP2D6 and CYP3A4

CYP	Substrate	$f_{m\mathrm{CYP}}$*	References
2C9	Tolbutamide	0.80	[16]
	S-warfarin	0.87	[10]
	Phenytoin	0.75	[17, 18]
2D6	Desipramine	0.88	See [7]
	Propafenone	0.76	
	Tolterodine	0.94	
	Encainide	0.86	
	Metoprolol	0.83	
	Mexiletine	0.49	
	Imipramine	0.46	
	Propranolol	0.37	
3A4	Midazolam	0.99, 0.94	[24–26]
	Triazolam	0.98, 0.92	[24]
	Alprazolam	0.80	[20]
	Nifedipine	0.71	[24, 27, 28]
	Nisoldipine	0.99	[27]
	Felodipine	0.99, 0.81	[24, 27, 29, 30]
	Quinidine	0.76	[21, 24, 27, 31]
	Simvastatin	0.99	[24]
	Lovastatin	0.99	[27, 32]

**When two values are shown, the higher value is derived from renal excretion data, whereas the lower value is obtained by regression/ranking and is that used in further predictions.*

16) to obtain an average $f_{m\mathrm{CYP}}$. Figure 2 shows the example of midazolam. The regression approach was also used for nifedipine and quinidine ($n = 5$ and 6). For the other CYP3A4 substrates (felodipine, nisoldipine, simvastatin and lovastatin) the number of studies available was more limited and $f_{m\mathrm{CYP}}$ values were obtained by ranking the AUC ratio (using either data from itraconazole or ketoconazole studies) relative to midazolam and applying this factor to the midazolam $f_{m\mathrm{CYP}}$. For the predictions of the AUC ratio the lower values of $f_{m\mathrm{CYP}}$ for the CYP3A4 substrates were used.

Data analysis

As described previously [6], the database analyses revealed that the inhibitor concentration was frequently not reported in an *in vivo* study, and when information was available in the same subjects, various concentrations were quoted (average, maximum or minimum). In order to standardize procedures, these concentrations were estimated from literature pharmacokinetic parameters. The average systemic plasma concentration after repeated oral administration ($[I]_{av}$), and the maximum hepatic input concentration ($[I]_{in}$) were calculated as in equations 4 and 3, respectively [9].

$$[I]_{av} = \frac{D/\tau}{CL/F} \tag{4}$$

In equation 4, F and τ represent the fraction of dose systemically available and dosing interval, respectively, of the inhibitor used in the *in vivo* interaction study. For the purpose of this analysis using equation 3, the f_a value was taken as 1, assuming that the inhibitors were completely absorbed from the gastrointestinal tract, the k_a value was initially assumed to be 0.1 min^{-1} (the maximum rate of gastric emptying) [9] and the blood-to-plasma concentration ratio and hepatic blood flow taken as unity and 1610 ml min^{-1}, respectively.

The $f_{m\mathrm{CYP}}$ data collected were incorporated into the prediction of AUC ratio using equation 2 for both $[I]_{av}$ and $[I]_{in}$ for all three CYPs and compared with initial *in vivo* predictions based on equation 1 for different $[I]$. In order to obtain more realistic k_a estimates, values were calculated for each inhibitor using the time to reach maximum plasma concentration ($T_{\max}$) and the elimination rate constant (k) as shown in equation 5 (the latter values collected from published literature data). For a number of inhibitors ($n = 5/10$ for CYP2C9, $n = 11/18$ for CYP2D6 and $n = 7/14$ for CYP3A4), this pharmacokinetic information was unavailable; therefore a value of 0.01 min^{-1} was assigned. The calculated k_a values for the inhibitors are listed in Table 2.

$$T_{\max} = \frac{\ln(k_a/k)}{(k_a - k)} \tag{5}$$

Refined k_a values (calculated from inhibitor pharmacokinetics or an assumed value of 0.01 min^{-1}) were incorporated into *in vivo* predictions for all three CYP enzymes for $[I]_{in}$, either alone or in combination with $f_{m\mathrm{CYP}}$ information, using equations 1 and 2, respectively. The success of prediction (within twofold of *in vivo* value) was compared with the previous database analysis ($f_{m\mathrm{CYP}} = 1$ and $k_a = 0.1$ min^{-1}). A twofold threshold value was selected on the basis of previous consensus reports [2, 11] for a significant

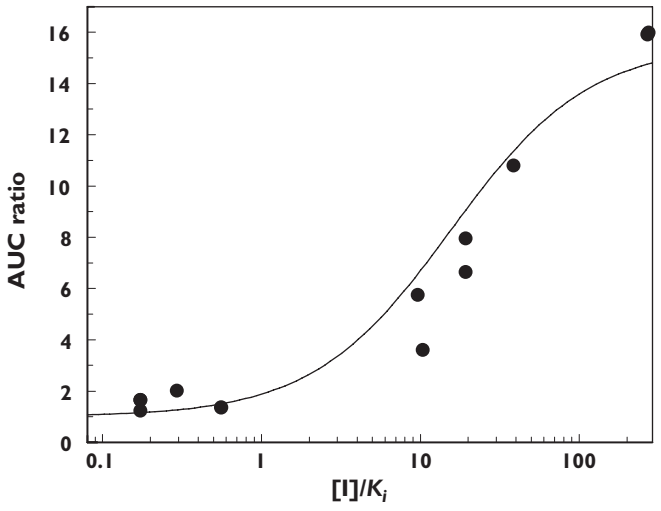

Figure 2

Determination of $f_{m\mathrm{CYP}}$ for midazolam. Relationship between the AUC ratio observed *in vivo* and $[I]_{in}/K_i$ ratio for 10 drug–drug interactions involving midazolam as the victim drug

Table 2

Absorption rate constants for CYP inhibitors involved in *in vivo* interaction studies

Inhibitor	CYP enzyme	k_a (min^{-1})	Reference
Sulphaphenazole	2C9	0.030	[9]
Fluconazole	2C9, 3A4	0.061	[33]
Ketoconazole	2C9, 3A4	0.013	[34]
Itraconazole	3A4	0.020	[35]
Quinidine	2D6, 3A4	0.014	[36]
Fluoxetine	2D6, 3A4	0.009	[37]
Fluvoxamine	2C9, 2D6, 3A4	0.008	[38]
Sertraline	2C9, 2D6	0.007	[37]
Citalopram	2D6	0.024	[37]
Nifedipine	3A4	0.056	[39]

increase in AUC ratio with a corresponding $[I]/K_i$ ratio of unity.

The $[I]/K_i$ ratio was calculated for each of the *in vivo* interaction studies using the various inhibitor concentrations described previously. Some inhibitors such as fluoxetine and itraconazole [6] have an active metabolite that also has inhibitory activity towards the same CYP enzyme. For these studies, the $[I]/K_i$ ratio was calculated for the both the parent and the metabolite, the values were then added [12]. Out of the three itraconazole metabolites reported by Isoherranen *et al.* [13] (hydroxy-, keto- and N-desalkyl-itraconazole), only the contribution of hydroxy-itraconazole was included in the prediction, consistent with the previous database analysis [6].

The change in AUC ratio *in vivo* was plotted against the AUC ratio predicted using the various parameters and predictions within twofold of the *in vivo* AUC ratio were considered successful. The bias of drug–drug interaction prediction was assessed from the geometric mean of the ratio of predicted and actual value (average-fold error, *afe*). The mean squared prediction error (*mse*) (difference between the predicted and observed *in vivo* value) and the root mean squared prediction error (*rmse*) provided a measure of precision for the prediction of the drug–drug interaction studies using including $[I]/K_i$, appropriate k_a and $f_{m\mathrm{CYP}}$ values, both individually and in combination [14, 15].

$$afe = 10^{\left|\frac{1}{n}\sum \log\frac{Predicted}{Observed}\right|} \tag{6}$$

$$mse = \frac{1}{n}\sum (Predicted - Observed)^2 \tag{7}$$

$$rmse = \sqrt{mse} \tag{8}$$

Results

From the original database [6] a subset of 115 studies was created for which $f_{m\mathrm{CYP}}$ data on the *in vivo* probe substrate were available. The drug–drug interaction studies selected ($n = 21$ for CYP2C9, $n = 40$ for CYP2D6 and $n = 54$ for CYP3A4) involved 23 different substrates and 42 inhibitors. The range of $f_{m\mathrm{CYP}}$ values was from 0.75 to 0.87 (CYP2C9), 0.37 to 0.94 (CYP2D6) and 0.71 to 0.99 (CYP3A4) (see Table 1). Figures 3 and 4 illustrate the effect of the $f_{m\mathrm{CYP}}$ values on the prediction of AUC ratio for 115 drug–drug interaction studies (based on equation 2) using either $[I]_{in}$ or $[I]_{av}$, respectively. The data in Figure 3A,B show that an improvement in the prediction accuracy is observed for each of the three CYP enzymes by incorporating the $f_{m\mathrm{CYP}}$ values for *in vivo* predictions based on the $[I]_{in.}$ The number of studies within the twofold range of the *in vivo* value increased by 24, 38 and 28% for CYP2C9, CYP2D6 and CYP3A4, respectively (Table 3) and there was a corresponding reduction in the bias and increase in precision.

Figure 4 indicates that the incorporation of $f_{m\mathrm{CYP}}$ data into the *in vivo* predictions based on $[I]_{av}$ has a similar but less substantial effect. The greatest improvement occurred for CYP2C9 with a 24% increase in the number of studies within the twofold limit of the *in vivo* value. Incorporation of $f_{m\mathrm{CYP}}$ data reduced several over-predictions for both CYP2D6 and CYP3A4. However, incorporation of $f_{m\mathrm{CYP}}$ for the $[I]_{av}$ prediction did not significantly improve the under-predictions obtained for CYP3A4 interactions; 30% of studies involving this enzyme were still classed as false-negative interactions (see Figure 4B).

The $[I]_{in}$ value represents the combination of the circulating systemic plasma concentration and the additional concentration occurring during the absorption phase. Figure 5 illustrates the relationship between the $[I]_{in}$ and $[I]_{av}$ values for the 115 data studies where k_a is assumed to be 0.1 min^{-1}. The contribution of the absorption term $k_a \cdot f_a \cdot D/Q_h$ to the slope of this relationship can be illustrated by considering three particular inhibitors (Table 4). Lowering the k_a value from the maximum value ($k_a = 0.1$ min^{-1}) to literature-reported values reduces the relative ratio between the absorption and systemic contribution by 10–13-fold for ketoconazole and itraconazole, but has a minimal effect for fluconazole. However, the dose absorbed is the main contributor to the high $[I]_{in}$ values and for $[I]_{av}$ this factor is less apparent due to the effect of volume of distribution.

Refinement of k_a values from literature information was possible for 10 inhibitors to provide new parameter values for 86 studies (Table 2); a ninefold range of k_a values was observed, ranging from 0.007 to 0.06 min^{-1} for sertraline and fluconazole, respectively. For the remaining studies involving inhibitors for which no absorption information was available, a k_a value of 0.01 min^{-1} was assigned as a reasonable estimate. Figure 3C shows the effect of incorporating these refined k_a values into *in vivo* predictions for 115 drug–drug interaction studies; $f_{m\mathrm{CYP}}$ was assumed to be 1 for these predictions. From the results in Figure 3 and Table 3, it can be seen that in comparison with the original analysis [6] where an arbitrary k_a of 0.1 min^{-1} was used, the k_a improves the prediction accuracy for all three CYP enzymes. The greatest effect was noted for CYP2D6, where a 25% increase in the number of studies within twofold of the *in vivo* value is observed. In

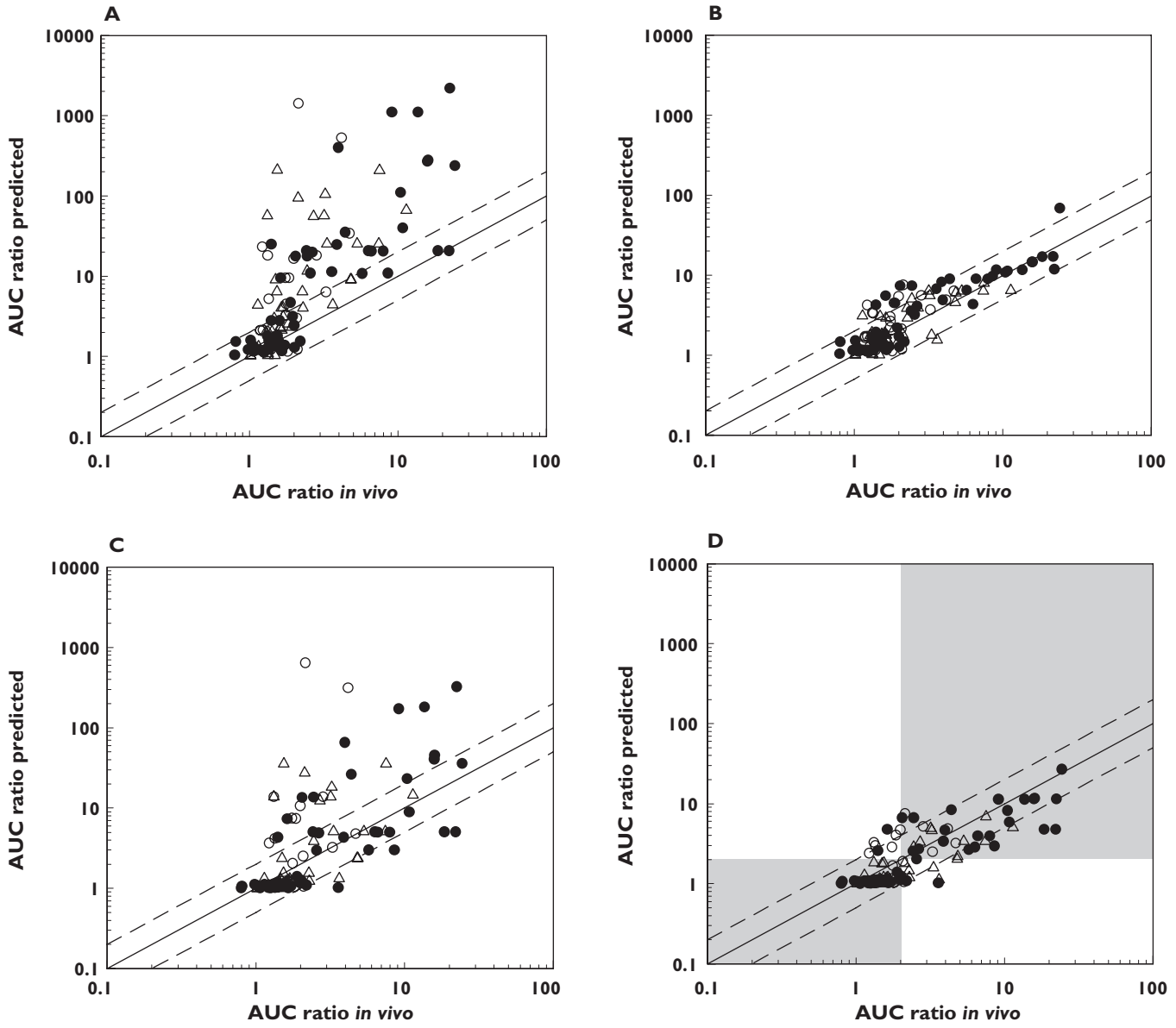

Figure 3

Relationship between the AUC ratio observed *in vivo* and the AUC ratio predicted for 115 drug–drug interaction studies involving CYP2C9 (○), CYP2D6 (△) and CYP3A4 (●). The plots represent predictions using the maximum hepatic input concentration—equation 1 (A), incorporating both the f_{mCYP}, equation 2 (B), refined k_a value (C) and both f_{mCYP} and k_a (D). Solid line represents line of unity, whereas dashed lines represent the twofold limit in prediction accuracy. The shaded areas represent the regions corresponding to negative and positive drug–drug interactions as defined by the borderlines of an AUC ratio of 2 and an $[I]/K_i$ of 1 [2]

addition, the use of refined k_a values significantly reduced the number of over-predictions in comparison with the higher k_a value (2.2- and 2.7-fold for CYP3A4 and CYP2D6 drug–drug interaction studies, respectively).

The incorporation of both f_{mCYP} and k_a resulted in the most successful prediction for all three CYPs, with a total of 81% of studies within twofold of the *in vivo* value (Figure 4D and Table 3). For these predictions, there was the least bias and improvement in precision, as judged by the statistical parameters *afe* and *rmse* (see Table 3).

Discussion

In a previous drug–drug interaction database analysis [6] we have shown the utility of $[I]_{in}$ in qualitative zoning of inhibitors, allowing the true negatives to be iden-

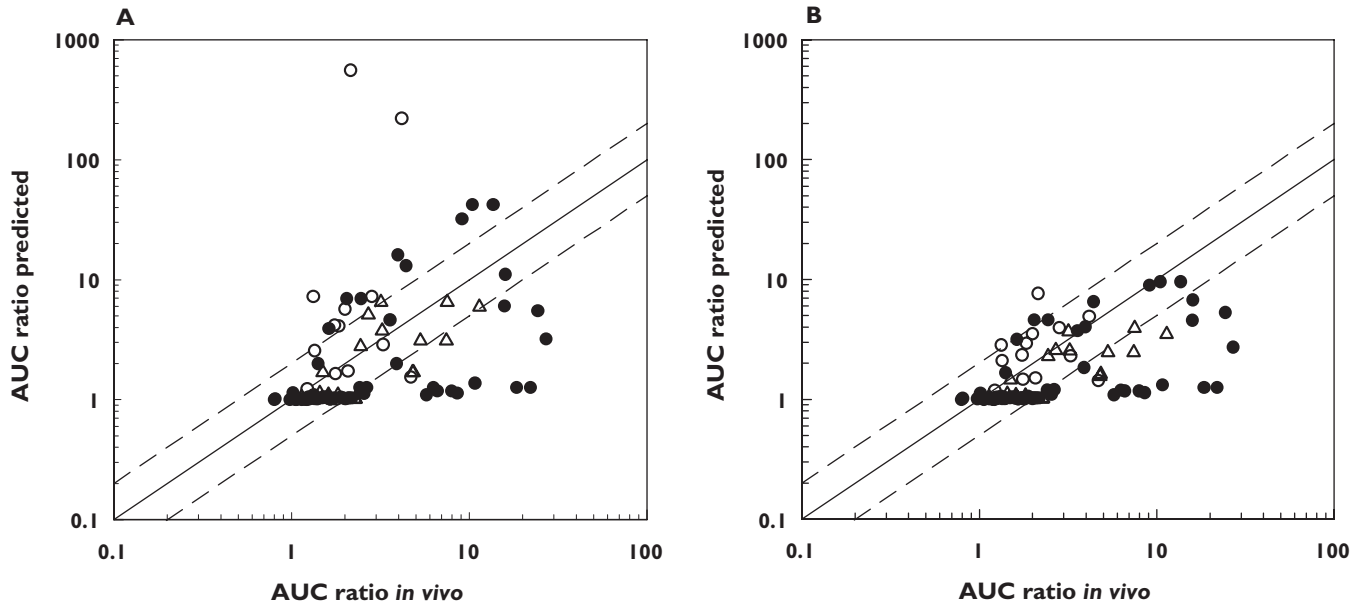

Figure 4

Relationship between the observed AUC ratio *in vivo* and AUC ratio predicted for 115 drug–drug interaction studies involving CYP2C9 (○), CYP2D6 (△) and CYP3A4 (●). The plots represent predictions using the average systemic total drug plasma concentration ($[I]_{av}$) (A), and incorporating f_{mCYP} data (B). The solid line represents line of unity, whereas dashed lines represent the twofold limit in prediction accuracy

Table 3

Prediction accuracy for 115 interaction studies illustrating the impact of f_{mCYP} and k_a parameters on the use of $[I]_{in}$ and *in vitro* K_i values. Number of studies for each CYP is shown together with the percentage success for the total number of studies

CYP	Prediction accuracy	$[I]_{in}$*	$[I]_{in}$ with f_{mCYP}	$[I]_{in}$ with refined k_a	$[I]_{in}$ with f_{mCYP} and refined k_a
2C9	Over-predictions	11	6	9	5
	Under-predictions	0	0	1	1
	Within twofold limit	10	15	11	15
2D6	Over-predictions	19	3	7	0
	Under-predictions	0	1	2	5
	Within twofold limit	21	36	31	35
3A4	Over-predictions	23	8	13	3
	Under-predictions	0	0	5	8
	Within twofold limit	31	46	36	43
Total	% within twofold limit	54	84	68	81
	afe	2.11	1.21	1.37	0.84
	rmse	144.2	4.8	75.6	2.95

*$f_{mCYP} = 1$ and $k_a = 0.1$ min^{-1}.

tified and eliminating false negatives. However, several false positives resulted and on a quantitative level the large over-prediction of true-positive effects was of concern (see Figure 1). The fact that this simple generic approach ignores specific substrate- or inhibitor-related properties no doubt contributes to a number of over-predictions of true-positive interactions. Therefore, this study focused on demonstrating the significance of f_{mCYP} for the victim drug (previously explored for CYP2D6 [7]) and k_a for the inhibitor on the drug–drug interaction prediction accuracy for 115 studies. In order to assess the impact of these particular parameters on the pre-

dicted AUC ratio, previously collated data were used [6], including the literature reported K_i values.

The range of $f_{m\mathrm{CYP}}$ values obtained for each CYP enzyme, 0.75–0.87 (CYP2C9), 0.37–0.94 (CYP2D6) and 0.71–0.99 (CYP3A4), illustrates that more than one enzyme/clearance mechanism contributes to the elimination of most of the victim drugs under consideration. The use of $f_{m\mathrm{CYP}}$ data in the assessment of AUC ratio corrected several false-positive predictions, as well as reducing the extent of over-predictions of true positives (Table 3). The improvement is most notable for the predictions using $[I]_{in}$, where the percentage of studies within the twofold limit of the *in vivo* AUC ratio increased from 54 to 84%.

Predictions for both CYP2C9 and CYP3A4 substrates are markedly improved to a comparable extent to that reported previously for CYP2D6 [7]. While $f_{m\mathrm{CYP}}$ values for the CYP2C9 substrates are relatively high, they are sufficiently less than 1 to benefit substantially from adopting equation 2 rather than equation 1. Incorporation of the renal clearance contribution for quinidine and alprazolam reduced the overestimation of the interactions with these CYP3A substrates by three- and 30-fold, respectively, whereas the impact of $f_{m\mathrm{CYP}}$ was of less significance for the other CYP3A4 substrates ($f_{m\mathrm{CYP}}$ range from 0.9 to 0.99). These findings extend the analysis on CYP2D6 substrates previously presented [7] and illustrate the general applicability of $f_{m\mathrm{CYP}}$ in progressing drug–drug interaction predictions to a valuable quantitative level.

A number of approaches were employed to obtain $f_{m\mathrm{CYP}}$ in this study. For all the CYP2D6 substrates, comparison of phenotyping data in extensive and poor metabolizers of CYP2D6 was used [7]. As previously discussed [7], the phenotyping approach will provide the most unequivocal method for establishing the importance of a particular cytochrome P450 in the clearance of a drug. A good alternative for polymorphic enzymes is 'phenocopying', that is from the difference between the urinary recovery of metabolites in both the presence and absence of a selective inhibitor. We were able to use this approach for the CYP2C9 substrate tolbutamide using sulphaphenazole [16]. For another CYP2C9 substrate phenytoin, it is known that CYP2C19 also contributes to its clearance [17] and the availability of phenotyping data allowed calculation of the contribution of the latter CYP [18] and hence a $f_{m\mathrm{CYP}}$ value for CYP2C9 and phenytoin. A $f_{m\mathrm{CYP}}$ value for CYP2C9 and warfarin has been estimated by Kunze and Trager [10] using a combination of information on the urinary recovery of metabolites, biliary excretion and the recovery of unchanged drug. This level of detail is not commonly available, even for probe substrates.

For CYP3A4 substrates, estimation of $f_{m\mathrm{CYP}}$ is problematic for several reasons, including the lack of selective inhibitors (ketoconazole and itraconazole being only selective at low concentrations) and com-

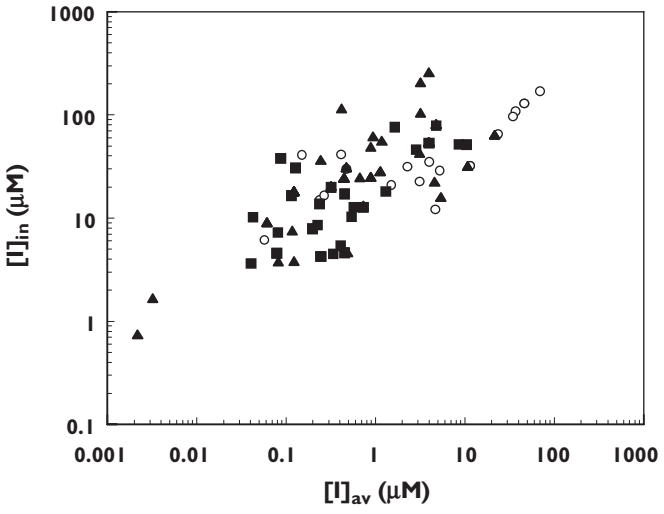

Figure 5
Relationship between $[I]_{in}$ and $[I]_{av}$ for 115 drug–drug interaction studies involving CYP2C9 (○), CYP2D6 (■) and CYP3A4 (▲)

Table 4
The effect of changing the k_a value on the ratio between the systemic and the absorption term ($k_a \cdot f_a \cdot D/Q_h$, equation 3) for ketoconazole, itraconazole and fluconazole

Inhibitor	$[I]_{av}$(μM)	k_a(min^{-1})	Absorption term (μM)	Absorption term/ systemic term
Ketoconazole	0.44	0.013	3.0	6.8
		0.1	23.4	53
Itraconazole	0.12	0.02	3.5	29
		0.1	17.6	147
Fluconazole	23.2	0.061	24.6	1.1
		0.1	40.55	1.7

plexities of multisite binding [19]. In this study, initial values were obtained from estimates of total metabolism calculated indirectly from urinary recovery of unchanged drug. These values are high (Table 1), which is consistent with the extensive use of several of these drugs (the benzodiazepines and calcium channel blockers) as selective probes. However, whether the metabolism of these substrates is completely mediated by CYP3A4 activity is debatable; thus these $f_{m\mathrm{CYP}}$ values should be regarded as upper estimates. In the cases of alprazolam and quinidine, the importance of renal clearance is well established [20, 21], resulting in $f_{m\mathrm{CYP}}$ values of ≤0.8. For the remaining seven substrates this method resulted in $f_{m\mathrm{CYP}}$ values of ≥0.98. Simulations using equation 2 have shown AUC ratios to be very sensitive to small changes in $f_{m\mathrm{CYP}}$ between values of 0.8 and 1 [7]; quinidine and alprazolam are the only CYP3A4 substrates outside this range. Most studies available used either midazolam, triazolam, alprazolam, quinidine or nifedipine, allowing a regression approach to be adopted based on equation 2 to obtain an average $f_{m\mathrm{CYP}}$ for these five drugs (see Figure 2 for midazolam). For quinidine and alprazolam there was good agreement between the regression and corrected renal excretion values. For felodipine, nisoldipine, simvastatin and lovastatin, due to the limited number of studies available, $f_{m\mathrm{CYP}}$ values were obtained by an alternative approach of ranking (either itraconazole or ketoconazole AUC ratios) relative to midazolam. Despite the limitations of these methods and the uncertainity of the absolute values of $f_{m\mathrm{CYP}}$ obtained for the CYP3A4, Figures 3 and 4 indicate good predictions for these substrates, comparable to those for CYP2C9 and CYP2D6.

Extending this work to drug–drug interactions involving victim drugs that are not established CYP probes will rely on an estimate of $f_{m\mathrm{CYP}}$. Most drugs have several enzymes contributing to their elimination and the key information needed is the relative importance of particular enzymes to those drug pathways, i.e. $f_{m\mathrm{CYP}}$ in contrast to the fraction metabolized by a particular pathway (often obtained via a radiolabel study). The importance of this type of specific information is being increasingly realized and various approaches have been recently summarized [11, 22]. The impact of hepatic transporters on drug clearance may also be an important consideration. However, the success apparent with CYP probe substrates described here, as well as theoretical relationships [7], would indicate that even approximate $f_{m\mathrm{CYP}}$ values may markedly improve a prediction.

The use of $[I]_{in}$ relies on an input term for the hepatic portal vein plasma concentration calculated from equation 3. Predictions based on these $[I]$ values, however, do result in a significant number of over-predictions or false-positive interactions [6]. One of the possible limitations of this approach is the use of the theoretical maximum value of 0.1 min^{-1} for the k_a, which represents the maximum rate of gastric emptying [9]. Refinement of this parameter resulted in the k_a values 2–14-fold lower than the initial estimates as shown in Table 2 for 10 CYP inhibitors investigated in the current study. Incorporation of refined k_a reduced the relative contribution of the absorption term in comparison to the systemic term in the $[I]_{in}$ value up to 13-fold, as illustrated for itraconazole in Table 4. In addition, the k_a value may vary with dose of inhibitor and the food intake (e.g. ketoconazole [23]), affecting the $[I]_{in}$ estimate and consequently the predicted AUC ratio.

Refined k_a values reduce the number of over-predictions observed for all three CYPs (Table 3). Predictions using $[I]_{in}$ when either a realistic k_a or $f_{m\mathrm{CYP}}$ value were incorporated individually predicted 68–84% of the interactions within twofold of *in vivo* value (comparable lack of bias). However, incorporation of $f_{m\mathrm{CYP}}$ improved the precision of the drug–drug interaction assessment (sevenfold lower *rmse*), substantially more than with the use of refined k_a values (see Table 3).

The use of $[I]_{in}$ incorporating both $f_{m\mathrm{CYP}}$ and refined k_a values resulted in the most successful prediction overall (see Figure 3D). A total of 81% of studies were within the twofold limit of the in vivo value and this represents an increase of 30% in comparison with the qualitative zoning assumptions ($k_a = 0.1$ min^{-1} and $f_{m\mathrm{CYP}} = 1$) previously described [6]. Minimal bias and high precision of the predictions were achieved (Table 3).

The accurate prediction of an *in vivo* drug–drug interaction is critically dependent on the inhibitor concentration used in equations 1 and 2. It is impossible to measure this concentration directly within the human liver and for this reason there are many conflicting reports about which inhibitor concentration to use in prediction, whether it is the systemic or portal vein concentration, total or unbound plasma concentration or the liver concentration. There have been many attempts to make an assessment of the concentration within the liver, with varying degrees of success [3, 9, 15]. Although in the present study the most successful predictions result from using a total drug concentration term ($[I]_{in}$) with $f_{m\mathrm{CYP}}$ and refined k_a values, there are still a number of falsely predicted interactions. The possibility of an interaction in the gut wall may be significant for certain substrates and has not been included in this approach. Another factor that can influence the *in vivo*

prediction is experimental variability in the generation of the *in vitro* data. The K_i values used in the current analysis are obtained from a variety of published literature sources and it would be valuable to explore whether standardization of the *in vitro* assessment would further improve prediction. This consideration is particularly pertinent for CYP3A4 K_i values, and a recent study has explored the importance of substrate selection and substitution for this enzyme [19].

In summary, we have demonstrated that incorporation of $f_{m\mathrm{CYP}}$ values for the victim drug markedly improves prediction of 115 drug–drug interactions compared with the use of the $[I]/K_i$ ratio alone. In addition to $f_{m\mathrm{CYP}}$, inclusion of realistic k_a values to refine estimates of $[I]_{in}$ provides the most useful estimate of $[I]$ and results in the most successful predictions as judged by a lack of bias and a high level of precision.

This work was funded by a consortium of pharmaceutical companies (AstraZeneca, Bristol Myers Squibb, GlaxoSmithKline, F. Hoffmann La Roche, Novartis, Pfizer and Servier) within the Centre for Applied Pharmacokinetic Research at the University of Manchester. H.S.B. was financially supported by a Bristol Myers Squibb studentship.

References

1 Ito K, Iwatsubo T, Kanamitsu S, Ueda K, Suzuki H, Sugiyama Y. Prediction of pharmacokinetic alterations caused by drug–drug interactions: metabolic interaction in the liver. Pharmacol Rev 1998; 50: 387–411.

2 Tucker GT, Houston JB, Hunag S-M. Optimising drug development: strategies to assess drug metabolism/transporter interaction potential–toward a consensus. Br J Clin Pharmacol 2001; 52: 107–17.

3 Von Moltke LL, Greenblatt DJ, Schmider J, Wright CE, Harmatz JS, Shader RI. In vitro approaches to predicting drug interactions in vivo. Biochem Pharmacol 1998; 55: 113–22.

4 Lin JH. Sense and nonsense in the prediction of drug–drug interactions. Curr Drug Metab 2000; 1: 305–31.

5 Yao C, Levy RH. Inhibition-based metabolic drug–drug interactions: predictions from in vitro data. J Pharm Sci 2002; 91: 1923–35.

6 Ito K, Brown HS, Houston JB. Database analyses for the prediction of in vivo drug–drug interactions from in vitro data. Br J Clin Pharmacol 2004; 57: 473–86. Erratum 58: 565–8.

7 Ito K, Hallifax D, Obach RS, Houston JB. Impact of parallel pathways of drug elimination and multiple CYP involvement on drug–drug interactions: CYP2D6 paradigm. Drug Metab Dispos 2005; 33: 837–44.

8 Rowland M, Matin SB. Kinetics of drug–drug interactions. J Pharmacokinet Biopharm 1973; 1: 553–67.

9 Kanamitsu SI, Ito K, Sugiyama Y. Quantitative prediction of in vivo drug–drug interactions from in vitro data based on physiological pharmacokinetics: use of maximum unbound concentration of inhibitor at the inlet to the liver. Pharm Res 2000; 17: 336–43.

10 Kunze KL, Trager WF. Warfarin–Fluconazole III. A rational approach to management of a metabolically based drug interaction. Drug Metab Dispos 1996; 24: 429–35.

11 Bjornsson TD, Callaghan JT, Einolf HJ, Fischer V, Gan L, Grimm S, Kao J, King SP, Miwa G, Ni L, Kumar G, McLeod J, Obach RS, Roberts S, Roe A, Shah A, Snikeris F, Sullivan JT, Tweedie D, Vega JM, Walsh J, Wrighton SA. The conduct of in vitro and in vivo drug–drug interaction studies: a pharmaceutical research and manufacturers of America (PhRMA) perspective. Drug Metab Dispos 2003; 31: 815–32.

12 Rostami-Hodjegan A, Tucker GT. 'In silico' simulations to assess the 'in vivo' consequences of 'in vitro' metabolic drug–drug interactions. Drug Discovery Today: Technologies 2004; 1: 441–8.

13 Isoherranen N, Kunze KL, Allen KE, Nelson WL, Thummel KE. Role of itraconazole metabolites in CYP3A4 inhibition. Drug Metab Dispos 2004; 32: 1121–31.

14 Sheiner LB, Beal SL. Some suggestions for measuring predictive performance. J Pharmacokinet Biopharm 1981; 9: 503–12.

15 Obach RS, Baxter JG, Liston TE, Silber BM, Jones BC, MacIntyre F, Rance DJ, Wastall P. The prediction of human pharmacokinetic parameters from preclinical and in vitro metabolism data. J Pharmacol Exp Ther 1997; 283: 46–58.

16 Back DJ, Orme ML'E. Genetic factors influencing the metabolism of tolbutamide. Pharmac Ther 1989; 44: 147–55.

17 Bajpai M, Roskos LK, Shen DD, Levy RH. Roles of cytochrome P4502C9 and Cytochrome P4502C19 in the stereoselective metabolism of phenytoin to its major metabolite. Drug Metab Dispos 1996; 24: 1401–3.

18 Fritz S, Lindner W, Roots I, Frey BM, Kupfer A. Stereochemistry of aromatic phenytoin hydroxylation in various drug hydroxylation phenotypes in humans. Pharmacol Exp Ther 1987; 241: 615–22.

19 Galetin A, Ito K, Hallifax D, Houston JB. CYP3A4 substrate selection and substituition in the prediction of potential drug–drug interactions. J Pharmacol Exp Ther 2005; 314: 180–90.

20 Garzone PD, Kroboth PD. Pharmacokinetics of the newer benzodiazepines. Clin Pharmacokinet 1989; 16: 337–64.

21 Ochs HR, Greenblatt DJ, Woo E. Clinical pharmacokinetics of quinidine. Clin Pharmacokinetics 1980; 5: 150–68.

22 Williams JA, Hurst SI, Bauman J, Jones BC, Hylan R, Gibbs JP, Obach RS, Ball SE. Reaction phenotyping in drug discovery: moving forward with confidence? Current Drug Metab 2003; 4: 527–34.

23 Daneshmend TK, Warnock DW, Ene MD, Johnson EM, Potten MR, Richardson MD, Williamson PJ. Influence of food on the pharmacokinetics of ketoconazole. Antimicrob Agents Chemother 1984; 25: 1–3.

24 Benet LZ, Oie S, Schwartz JB. Design and optimisation of dosage regimens; pharmacokinetic data. In: Goodman and Gilman's the pharmacological basis of therapeutics, 10th edn, eds Hardman JG, Limbird LE. New York: McGraw-Hill 2001.

25 McCrea J, Prueksaritanont T, Gertz BJ, Carides A, Gillen L, Antenello S, Brucker MJ, Mileer-Stein C, Osborne B, Waldman S. Concurrent administration of the erythromycin breath test (EBT) and oral midazolam as in vivo probes for CYP3A activity. J Clin Pharmacol 1999; 39: 1212–20.

26 Smith MT, Eadie MJ, Brophy TO. The pharmacokinetics of midazolam in man. Eur J Clin Pharmacol 1981; 19: 271–8.

27 Physicians Desk Reference. Montvale, NJ: Medical Economics 2003.

28 Sorkin EM, Clissold SP, Brogden RN. Nifedipine. A review of its pharmacodynamic and pharmacokinetic properties, and therapeutic efficacy, in ischaemic heart disease, hypertension and related cardiovascular diseases. Drugs 1985; 30: 182–274.

29 Dunselman PH, Edgar B. Felodipine clinical pharmacokinetics. Clin Pharmacokinet 1991; 21: 418–30.

30 Edgar B, Regardh CG, Johnsson G, Johansson L, Lundborg P, Lofberg I, Ronn O. Felodipine kinetics in healthy men. Clin Pharmacol Ther 1985; 38: 205–11.

31 Brosen K, Davidsen F, Gram LF. Quinidine kinetics after a single oral dose in relation to the sparteine oxidation polymorphism in man. Br J Clin Pharmacol 1990; 29: 248–53.

32 Desager JP, Horsmana Y. Clinical pharmacokinetics of 3-hydroxy-3-methylglutaryl-coenzyme A reductase inhibitors. Clin Pharmacokinet 1996; 31: 348–71.

33 Debruyne D, Ryckelynck JP. Clinical pharmacokinetics of fluconazole. Clin Pharmacokinet 1993; 24: 10–27.

34 Daneshmend TK, Warnock DW, Turner A. Pharmacokinetics of ketoconazole in normal subjects. J Antimicrob Chemother 1981; 8: 299–304.

35 Hardin JC, Graybill JR, Fetchick R, Woestenborghs R, Rinaldi MG, Kuhn JG. Pharmacokinetics of itraconazole following oral administration to normal volunteers. Antimicrob Agents Chemother 1988; 32: 1310–3.

36 Greenblatt DJ, Pfeifer HJ, Ochs HR, Franke K, MacLaughlin D, Smith TW, Koch-Weser J. Pharmacokinetics of quinidine in humans after intravenous, intramuscular and oral administration. J Pharmacol Exp Ther 1977; 202: 365–78.

37 Van Harten J. Clinical pharmacokinetics of selective serotonin reuptake inhibitors. Clin Pharmacokinet 1993; 24: 203–20.

38 Gatti G, Spina E. Clinical pharmacokinetics of fluvoxamine. Clin Pharmacokinet 1994; 27: 175–90.

39 Kleinbloesem CH, van Brummelen P, van de Linde JA, Voogd PJ, Breimer DD. Nifedipine: kinetics and dynamics in healthy subjects. Clin Pharmacol Ther 1984; 35: 742–9.